Redox nanoparticles inhibit oxidative degradation of chemotherapeutic drugs and enhance its therapeutic effect in prostate cancer

Sindhu Thangavel
Doctoral Program in Materials Science
Student ID Number: 201130118
Doctor of Philosophy in Engineering
Advised by Professor Yukio Nagasaki
Signature

1. Introduction

Prostate cancer is the most prevalent type of malignancy and is the sixth major cause of death in males worldwide. Although survival rates are improving, there is always a risk of acquired chemo-resistance, relapse, and metastasis. Prostate cancer initially develops as an androgen dependent malignancy, but it soon progresses to an androgen independent stage via androgen ablation therapy and tolerance to chemotherapy [1]. Therefore, alternative treatment strategies are required to effectively inhibit cell growth and induce cell death in hormone-resistant prostate cancer accompanied by no toxicity in normal tissues.

Curcumin is a phytochemical with versatile biological characteristics, which include anti-inflammatory, anti-oxidant, and anti-tumor properties that induce cell death in various types of cancer cell lines [2] including androgen dependent and independent prostate cancer cell lines [3]. Although many molecular targets of curcumin have been extensively studied, identifying its targets in the chemo-resistant prostate cancer PC-3 cell line is important, because proteins are differentially targeted based on the type of malignancy [4]. For example, acid ceramidase is an enzyme which catalyzes the hydrolysis of ceramides and has received much attention recently as a potential therapeutic target, because of its elevated expression, particularly in prostate cancer cells [5]. While few studies have demonstrated curcumin's role in increasing ceramide levels in cancer cells, acid ceramidase has not yet been identified as a target of curcumin in prostate cancer and requires further investigation. Most of curcumin's promising therapeutic effects have been observed *in vitro*, while its efficiency *in vivo* is usually inadequate and does not reflect the *in vitro* results. Many clinical trials involving curcumin have been carried out on small groups of patients, and limited success has been achieved, mainly because of its low bioavailability [6, 7]. One of the key factors causing low bioavailability may be the spontaneous oxidative degradation of curcumin *in vivo* [8]. Curcumin undergoes oxidation at physiological conditions [9] in which two oxygen molecules are included into the heptadienone chain connecting the curcumin phenolic rings resulting in the formation of dioxygenated bicyclopentadione product [8-10]. The oxidative degradation of curcumin is a consequence of its activity as an ROS scavenger; thus, its antioxidant activity precludes it from exerting its role as an anti-tumor drug. For this reason, mixing curcumin together with low molecular weight (LMW) antioxidants can slow curcumin oxidation and consequently, increase its anti-tumor efficacy *in vitro* [11]. However, if a LMW antioxidant and curcumin are administered simultaneously, curcumin might still rapidly degrade *in vivo* because both compounds would diffuse throughout the body and would not be in close vicinity. In addition, high concentrations of LMW antioxidants are known to be internalized into not only cancer cells but also normal cells, which can cause homeostatic disturbances in healthy cells and result in adverse effects [12, 13].

Drug delivery systems (DDS) such as liposomes or polymer based nanoparticles are promising approaches for targeted drug delivery [14]. So far, various drug carriers have been reported to successfully encapsulate curcumin, improve its solubility, prevent its degradation by minimizing exposure to the aqueous medium, and deliver it to the tumor site by the enhanced permeability and retention (EPR) effect [15, 16]. Nonetheless, because conventional nanoparticles lack ROS-scavenging activity, they cannot protect curcumin from oxidative degradation caused by ROS and peroxidases, which are present at elevated levels in most tumor types, including prostate cancer [17].

To prevent curcumin oxidative degradation, we designed a unique ROS-scavenging polymeric micelle, referred to as pH-sensitive redox nanoparticle (RNP^N), that is prepared by self-assembling amphiphilic block copolymers with nitroxide radicals (**see Figure 1A**). The nitroxide radical compound used here is 2, 2, 6, 6-tetramethylpiperidine-1-oxyl (abbreviated as "TEMPO"), which is one of the strongest antioxidants. In our previous study, we confirmed that pH-sensitive RNP^N accumulates in tumor regions by the EPR effect [18] and disintegrates in tumor sites in response to low pH [19], thus increasing therapeutic efficiency.

In this paper, curcumin was encapsulated in the core of RNP^N (curcumin@RNP^N). We evaluated the stability of encapsulated curcumin in various oxidative conditions and investigated if curcumin@RNP^N could induce apoptosis in the androgen independent PC-3 prostate cancer cell line. In addition, the therapeutic efficiency of intravenously administered curcumin@RNP^N was explored *in vivo* in PC-3 tumor-bearing mice.
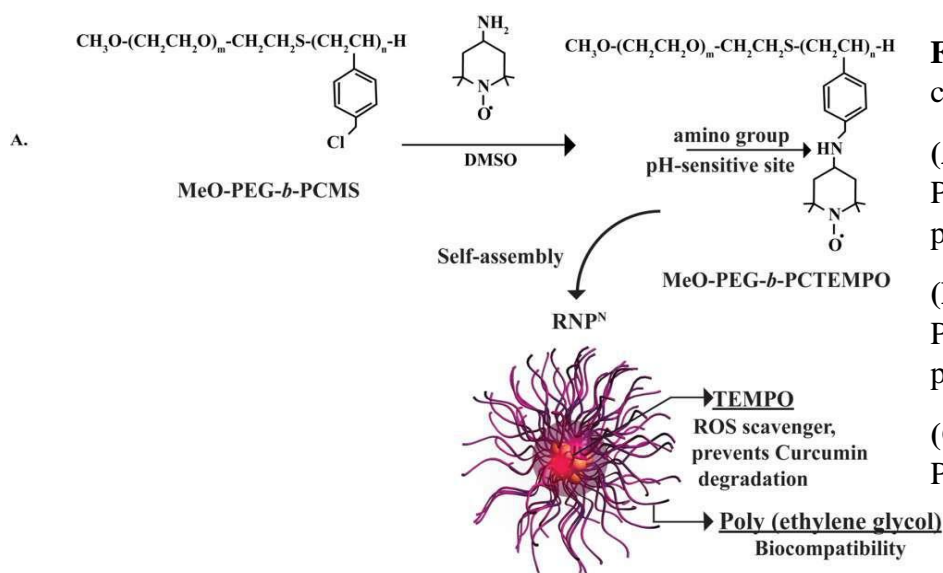
Figure 1: Synthesis and characterization of redox polymer

(A) Synthesis schemed of MEO-PEG-*b*-PCTEMPO and preparation of RNP^N.

(B) ^{1}H NMR spectrum of MEO-PEG-*b*-PCTEMPO in presence of phenylhydrazine.

(C) SEC spectra of MEO-PEG-*b*-PCMS.
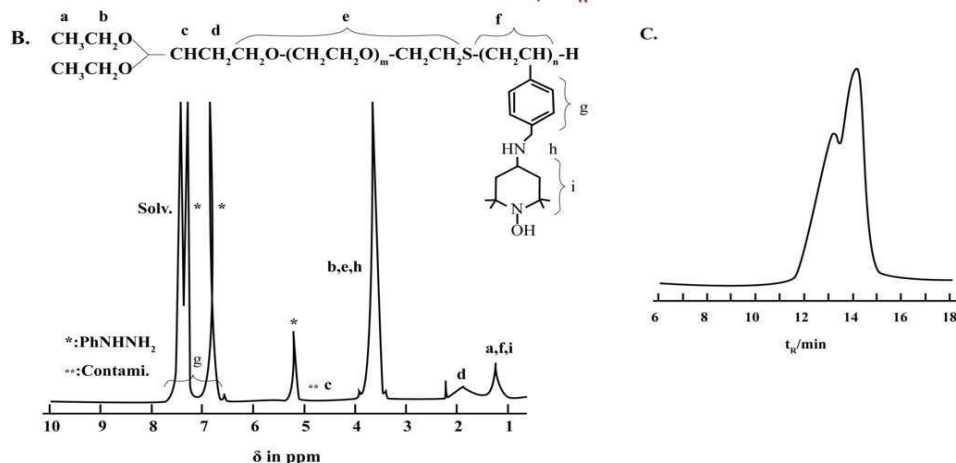
2. Preparation of curcumin loaded redox nanoparticle

RNP^N was prepared by a self-assembling MeO-PEG-*b*-PMNT block copolymer (**Figure 1A**). Briefly, methoxy-poly(ethylene glycol)-*b*-poly(chloromethylstyrene) (MeO-PEG-*b*-PCMS) was synthesized by the radical telomerization of chloromethylstyrene (CMS) using methoxy-poly(ethylene glycol)-suphanyl (MeO-PEG-SH; Mn = 5,000) as a telogen. Unit number of PCMS was 16. The chloromethyl groups on the PCMS segment of the block copolymer MeO-PEG-*b*-PCMS were converted to stable radical via amination of MeO-PEG-*b*-PCMS with 4-amino-TEMPO in dimethysulfoxide (DMSO). After the purification of the obtained PEG-*b*-PCTEMPO, the substitution ratio of the modified TEMPO moieties per repeating unit of PCMS was 80%, as determined by EPRR spectroscopy using the standard curve of free-amino-TEMPO in chloroform. The PEG-*b*-PCTEMPO was then dialyzed against water to obtain RNP^N. The NMR and SEC characteristics are illustrated in **Figures 1B and 1C**. For curcumin encapsulation, PEG-*b*-PCTEMPO and curcumin were mixed in DMF and then dialyzed against water to obtain curcumin@RNP^N.

3. Curcumin oxidative degradation in suppressed by RNP^N

One of the primary reasons for curcumin encapsulation was to minimize its oxidative degradation in physiological conditions. We compared the stability of curcumin@RNP^N with that of free curcumin, a mixture of curcumin and LMW TEMPOL, and curcumin encapsulated in control, PEG-b-PLA micelles and PEG-b-PCHMS micelles. **Figure 2A** shows curcumin's stability in culture medium with 10% fetal bovine serum (FBS). About 55% of free curcumin was degraded in 6 h in FBS containing medium. Curcumin in the control micelles exhibited higher stability than free curcumin due to its encapsulation in the hydrophobic core. However, curcumin degradation was still observed when it was rapidly released into aqueous solution at 37 °C (discussed in the next section) from control nanoparticles.
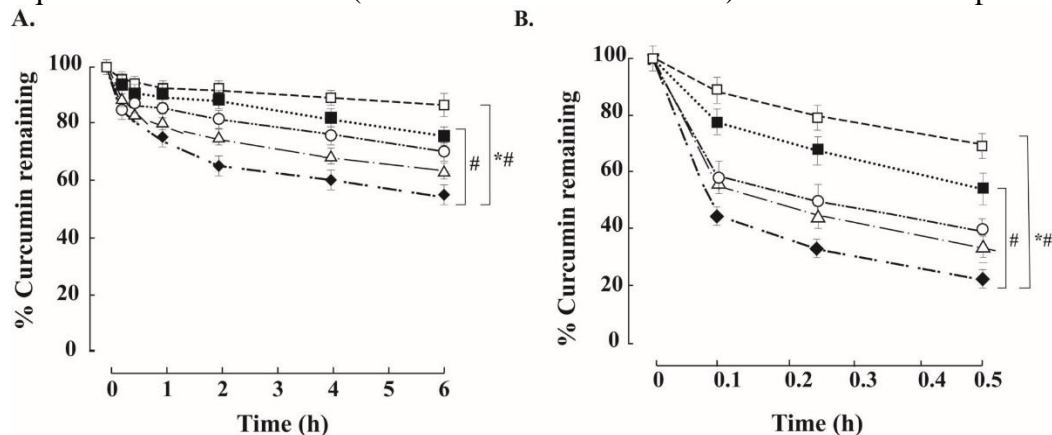
Figure 2: (A) Stability of curcumin in culture medium with 10% FBS. **(B)** Stability of curcumin under superoxide generated by xanthine (0.5 mmol/L)-xanthine oxidase (0.5 U/mL) reaction. Free curcumin (closed rhombus), mixture of free curcumin and TEMPOL (closed square), curcumin@RNP^N (open square), curcumin@PEG-*b*-PLA micelle (open triangle), and curcumin@PEG-*b*-PCHMS micelle (open circle). #p<0.05 compared with control, *p<0.001 compared with curcumin@RNP^N to all other groups. The data are presented as mean ± SD (n = 3).

The addition of TEMPOL significantly suppressed degradation by scavenging free radicals formed during this experiment. Degradation of curcumin was significantly suppressed by encapsulating both TEMPO and curcumin in the core of RNP^N probably because the local concentration of TEMPO was higher around curcumin due to encapsulation, which is a sharp contrast to mixing LMW TEMPOL with curcumin. Curcumin's oxidative degradation was known to be accelerated in the presence of free

radicals, due to its activity as an antioxidant, due to which, delivery of intact curcumin to target sites was decreased. **Figure 2B** shows the stability of curcumin in the presence of xanthine-xanthine oxidase reaction-generated superoxide [21]. About 80% of free curcumin degraded within 30 min, demonstrating that exogenous ROS accelerated curcumin's degradation in aqueous buffer. The curcumin@PEG-*b*-PLA micelle and curcumin@PEG-*b*-PCHMS micelle groups did not offer any protection for curcumin because gaseous superoxide can penetrate through the nanoparticle core to induce curcumin oxidative degradation. In contrast, due to increased local concentration of TEMPO by encapsulation in RNP^N with curcumin, we demonstrated remarkable suppression of curcumin oxidative degradation and about 70% of the curcumin remained intact even at higher xanthine concentrations. Therefore, RNP^N offers a sophisticated solution for the prevention of curcumin oxidative degradation through its TEMPO moiety radical scavenging activity, which is absent in control micelles.

4. *In vitro* drug release profile of curcumin@RNP^N

The PMNT segment of PEG-*b*-PMNT possesses both a hydrophobic phenyl group and an amino group in each repeating unit, RNP^N disintegrates in response to acidic pH, owing to the protonation of the amino groups [20]. Therefore, the release profiles of curcumin from nanoparticles were evaluated at different pHs ranging from neutral to acidic conditions at 37 °C. The drug release from curcumin@RNP^N at pH 7.4 was slower and 60% of the curcumin remained encapsulated even at 72 h (**Figure 3A**). Due to the protonation of amino groups in the hydrophobic core of RNP^N, rapid drug release was observed at pH 6.0 and about 60% of the curcumin was released in 24 h. Under more acidic condition (pH 2.4), a burst release of about 70% of the curcumin was observed within 2 h. In contrast, both curcumin@PEG-*b*-PLA micelles and curcumin@PEG-*b*-PCHMS micelles exhibited a rapid initial burst release (> 50%) of the encapsulated curcumin within 2 h (see **Figure 3B**) at pH 7.4. It has been reported that a favorable interaction between the drug and the polymeric micelle decreases the rate of drug diffusion, and the drug release depends on the rate of diffusion [21]. This might explain the rapid release pattern of the control micelles. The release profile of curcumin from RNP^N at pH 6.0 is more clinically relevant because it mimics the pH in the tumor microenvironment and curcumin is anticipated to be released in the extracellular region of the tumor.
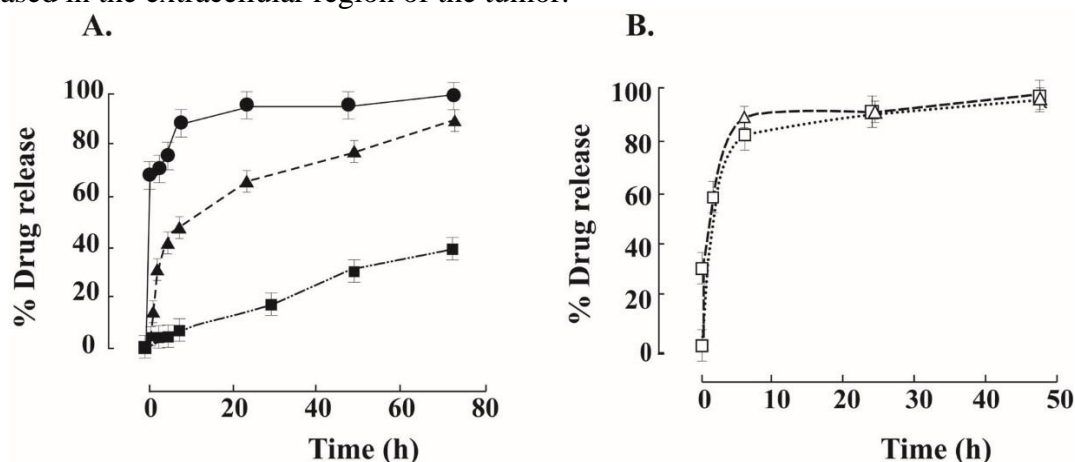
Figure 3: (A) Time- and pH- dependent curcumin release profiles of curcumin@RNP^N in phosphate buffered saline (PBS) (pH 7.4) (closed square), PBS (pH 6.0) (closed triangle) and acetate buffered saline (pH 2.4) (closed circle). **(B)** Time-dependent curcumin release profiles of curcumin@PEG-*b*-PLA micelle (open square) and curcumin@PEG-*b*-PCHMS micelle (open triangle) in PBS (pH 7.4). The data are presented as mean ± SD (n = 3).

5. *In vitro* cytotoxicity and drug uptake of curcumin@RNP^N in PC-3 cell lines

Since we established that curcumin stability could be enhanced by entrapment in RNP^N, its cytotoxicity and internalization in prostate cancer cells were investigated. Its cytotoxicity *in vitro* was tested on PC-3 prostate cancer cell lines by MTT cell viability assay. As shown in **Figure 4A**, dose-dependent cell viabilities were observed in PC-3 cells treated with curcumin, RNP^N, and curcumin@RNP^N. Cells treated with RNP^N alone showed a non-significant cytotoxicity even at higher concentrations, which corresponds with our previous report [22].
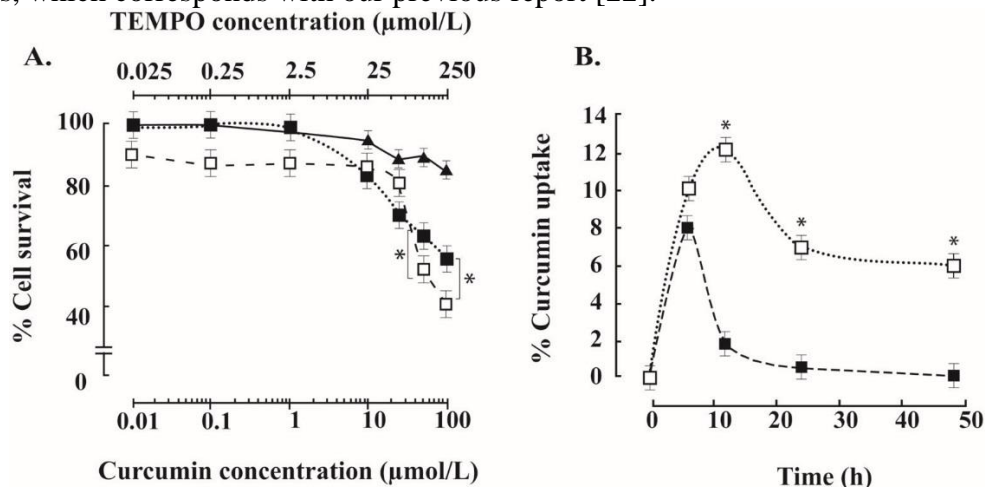
Figure 4: (A) Concentration dependent cytotoxicity of curcumin (closed square), curcumin@RNP^N (open square) and RNP^N (closed triangle) in PC-3 cell line as measured by MTT assay at 48h. The data are presented as mean ± SD (n = 3). *p<0.05 compared with free curcumin. **(B)** Time-dependent cellular uptake in PC-3 cell line quantified by LC/MS. Curcumin (closed square) and curcumin@RNP^N (open square). The data are presented as mean ± SD (n = 3). *p<0.001 compared with free curcumin.

Curcumin reduced cell survival by 60% at 100 µmol/L; therefore, the IC$_{50}$ of both curcumin and void RNP^N was above the concentrations tested in this study. Higher curcumin concentrations were required to induce cytotoxicity in cell lines because of its tendency to degrade in the culture medium. In contrast, curcumin@RNP^N significantly enhanced cytotoxicity compared to free curcumin and RNP^N. The IC$_{50}$ of curcumin@RNP^N was 50 ± 5.5 µmol/L at 48 h, which was at least 2-fold less as compared to free curcumin. Since curcumin remained stably encapsulated in RNP^N in culture medium, even at lower concentrations, a cytotoxic profile was observed, and IC$_{50}$ values were significantly decreased. To further confirm the effect of curcumin encapsulation in RNP^N on cellular uptake, we analyzed the percentage of curcumin uptake by LC/MS. PC-3 cells treated with free curcumin showed only about 8% uptake at 6 h and uptake was gradually decreased to untraceable limits with increasing time. In contrast, cells treated with curcumin@RNP^N exhibited about 10% of curcumin uptake at 6 h, which increased to 12% at 12 h. Even at the end of 48 h, about 7% of curcumin was still detected in the cells (**Figure 4B**). In our previous study, we reported that the pH-triggered release of entrapped drug from polymeric micelles is an important factor for increasing cellular uptake because it avoids drug efflux by P-glycoprotein located in the cellular membrane of cancer cells [23]. Possibly, the same mechanism might play a role in the enhanced cellular uptake observed in curcumin@RNP^N-treated cells. In addition, as shown in **Figure 2A**, curcumin is rapidly degraded in culture medium which accounts for the low

cell uptake observed here. Since RNP^N increased the stability of curcumin, even after 48 h, cellular uptake in those cells remained high.

6. Inhibition of ROS and nuclear factor kappa-light-chain-enhancer of activated B cells (NF-κB) activation by curcumin@RNP^N

RNP^N contains TEMPO, a strong ROS scavenger and curcumin is also a natural antioxidant. Therefore, we investigated the effect of RNP^N and curcumin on ROS-scavenging in the cells by double staining treated cells with the ROS-sensitive fluorescent dye 5-(and 6)-chloromethy-2,7-dichlorodihydrofluorescein diacetate (CM-H$_2$DCFDA; green) to examine ROS levels and mitotracker red chloromethyl-X-rosamine (CMXRos; red) to measure the change in mitochondrial membrane potential simultaneously.
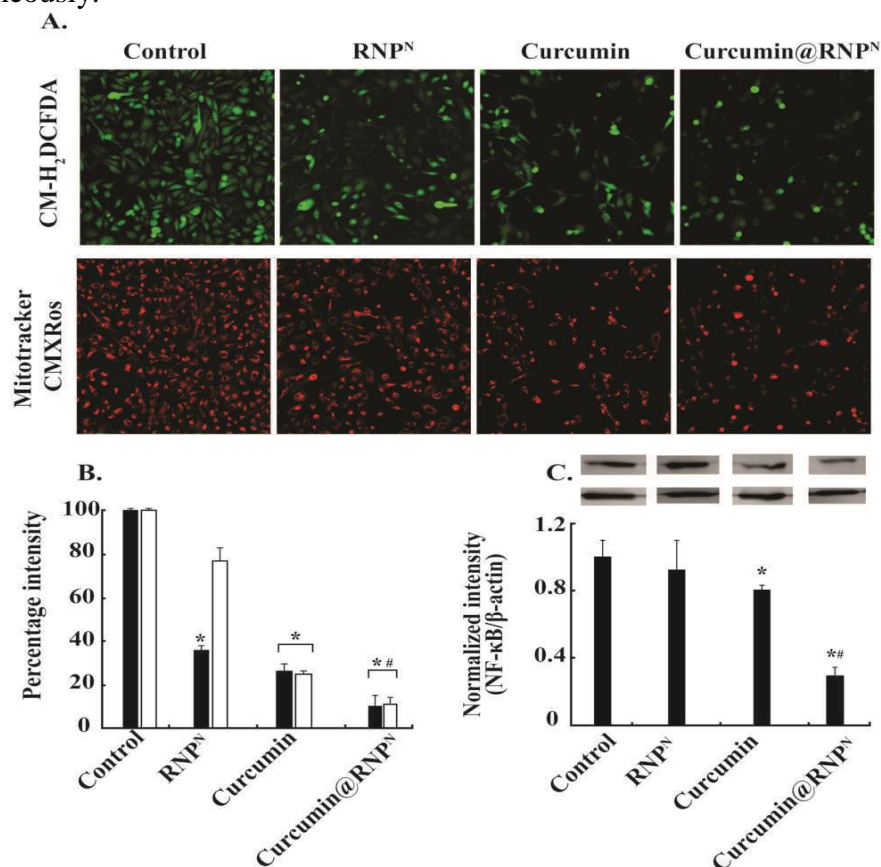
Figure 5: (A) Confocal fluorescence microscopy images of cells stained with 10 μmol/L ROS-sensitive dye CM-H$_2$DCFDA and 20 nmol/L mitotracker CMXRos red to visualize ROS and mitochondrial membrane potential, respectively. The differential interference contrast image (DIC) is shown in Figure S3. **(B)** The percentage intensities of CM-H$_2$DCFDA (black bar) and mitotracker CMXRos red (white bar) are normalized to cell number counted. The percentage intensities presented as mean ± SD (n = 3). *p<0.001 compared with control #p<0.05 compared with free curcumin. **(C)** Suppression of NF-κB expression in prostate cancer cell line PC-3 quantified by Western blot. *p<0.05 compared with control #p<0.05 compared with free curcumin. The normalized intensities presented as mean ± SD (n = 3). (The original western blots are shown in supporting data Figure S4).

Non-treated cells exhibited high green fluorescence, and clear mitochondrial red localization indicating higher ROS levels and healthy viable mitochondria (**Figure 5A**). The quantitative fluorescence intensity data of CM-H$_2$DCFDA and mitotracker CMXRos are shown in **Figure 5B**. RNP^N-treated cells displayed significantly decreased ROS levels, but a marginal loss in mitochondrial membrane potential was also observed. These data indicate that RNP^N and its disintegrated polymers do not cause any strong disturbance in mitochondrial function. In contrast, cells treated with curcumin showed reduced ROS levels and mitochondrial membrane potential, which is a typical effect of LMW antioxidants. Curcumin@RNP^N treated cells showed significant decrease in ROS levels and increased mitochondrial damage compared to both RNP^N and free curcumin. The significant mitochondrial membrane damage by curcumin@RNP^N resulted from the enhanced uptake of intact curcumin due to its encapsulation in RNP^N. Increased oxidative stress has been linked to NF-κB activation, which causes increased cancer cell resistance to apoptosis [24] and is often upregulated in prostate cancer cells [25]. Therefore, NF-κB is a potential target for prostate cancer. Quantification of nuclear protein expression levels by Western blot (see **Figure 5C**) revealed a modest suppression of NF-κB expression by curcumin and RNP^N alone, while curcumin@RNP^N significantly suppressed NF-κB expression.
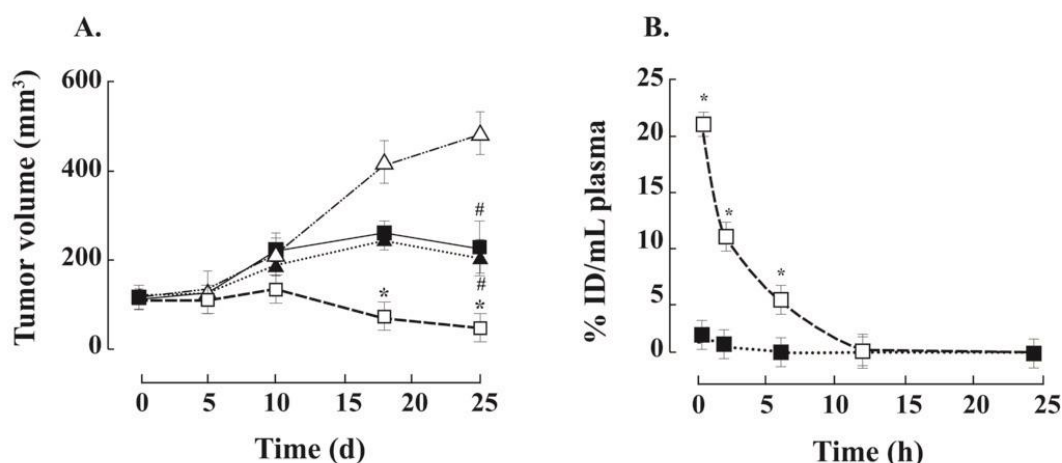
Figure 6: (A) Effect of free curcumin and curcumin@RNP^N in BALB/c nude mice bearing PC-3 tumors. Animals were intravenously administered with PBS (open triangle), free curcumin (10 mg/kg) (closed triangle) RNP^N (20 mg/kg) (closed square) and curcumin@RNP^N (10 mg/kg of curcumin, 20 mg/kg of RNP^N) (open square). Tumor growth was significantly inhibited by curcumin@RNP^N, in comparison to free curcumin and RNP^N. *p<0.05 compared with control, #p<0.01 compared with free curcumin. Tumor volume is expressed as mean ± SD (n = 5). **(B)** Distribution profile of curcumin (closed square) and curcumin@RNP^N (open square) in blood expressed as percentage injected dose, %ID/mL plasma. The mice was intravenously injected with 10 mg/kg equivalent curcumin. *p<0.001 compared with free curcumin. The data are presented as mean ± SD (n = 5). The chromatograms of curcumin detected in plasma are shown in supplementary Figure S8.

7. Therapeutic efficiency of curcumin@RNP^N *in vivo*

To confirm the anti-cancer potential of curcumin@RNP^N *in vivo*, free curcumin, RNP^N, and curcumin@RNP^N were administered to tumor-bearing nude mice intravenously via the tail vein. Both curcumin and RNP^N treated mice displayed reduced tumor volume compared to control mice, but no significant difference was observed between the two (see **Figure 6A**). In contrast, curcumin@RNP^N-treated mice exhibited a significant reduction in tumor volume growth rate. The enhanced stability of curcumin by RNP^N resulted in an increased plasma curcumin concentration in curcumin@RNP^N-treated mice. About 22% of the injected dose/mL plasma was detected 30 min after intravenous

curcumin@RNP^N injection, and a significant amount of curcumin was detected even after 6 h. Mice treated with curcumin displayed only 1-2.5% of the injected dose/mL plasma after 30 min and no curcumin peaks were detected after 2 h (**Figure 6B**). Since the anti-cancer activity of curcumin@RNP^N was directly proportional to the extent of ROS scavenging at target sites according to our *in vitro* results, we investigated whether curcumin@RNP^N suppressed oxidative stress at the tumor site after intravenous administration. We also observed that curcumin@RNP^N-treated mice significantly suppressed the superoxides and lipid peroxidation in tumor tissues compared to free curcumin- and RNP^N-treated mice. From the *in vitro* results, we can comprehend that after intravenous administration of curcumin@RNP^N, intact curcumin was delivered into tumor sites, leading to increase apoptosis and cell death.

8. RNP^N increase the bioavailability and suppress the side effects caused by pioglitazone

Pioglitazone is a member of the thiazolidinediones (TZD) class of drugs, generally used as insulin sensitizers has also been shown to exhibit potential anti-tumor properties, however, its exact molecular mechanisms has not been clearly elucidated. In addition, pioglitazone association with liver toxicity, cardiac abnormalities, and increase in body weight, restricted its application for therapeutic purposes. In this study, we addressed these issues by encapsulating pioglitazone in a radical scavenging nanoparticle (RNP^N). From *in vitro* experiments we elucidated that the molecular mechanisms leading to cell death was via both apoptosis and cell cycle arrest. Both *in vivo* and *in vitro* studies show pioglitazone metabolism in liver forms reactive oxidative intermediates[26] and leads to increased reactive oxygen species (ROS) generation, potentially causing damage in the hepatocytes, thus injuring the liver. In this study, mice administered with pioglitazone showed damage in liver sinusoids. This was significantly minimized by administration of Pioglitazone loaded RNP^N. Therefore, RNP^N in addition to increasing the bioavailability and therapeutic efficiency of drug, it adverted the toxic side effects of Pioglitazone.

9. Discussion and conclusions

Many therapeutic drugs available of chemotherapy are also known to exhibit side effects, most of which is caused due to increased oxidative stress. Consecutively, use of antioxidant drugs as an anti-tumor drug also proved to be in vain, due to their rapid oxidative degradation in presence of ROS which is found in high levels in tumor micro-environment. In this study, we explored and presented a suitable strategy to address both these issues. Curcumin is a highly unstable drug which undergoes spontaneous oxidative degradation even in physiological conditions. Curcumin loaded RNP^N prevented oxidative degradation consequently increasing its therapeutic efficiency.

We also investigated the effect of encapsulating pioglitazone, a potent anti-cancer drug with side effects causing liver injury. RNP^N combination treatment successfully repressed the liver injury. In addition, cellular drug uptake was increased in PC-3 prostate cancer cells *in vitro* and also in tumor areas *in vivo*. A detailed molecular mechanism of cell toxicity was investigated for both these drugs in PC-3 prostate cancer cell lines. Based on these results, RNP^N is a promising therapeutic intervention, for drugs prone to oxidation and for drugs which induce oxidative stress related side effects.

References
[1] J.T. Isaacs, The biology of hormone refractory prostate cancer. Why does it develop?, Urol Clin North Am, 26 (1999) 263-273.
[2] B.B. Aggarwal, C. Sundaram, N. Malani, H. Ichikawa, Curcumin: the Indian solid gold, Adv Exp Med Biol, 595 (2007) 1-75.

[3] S. Shankar, Q. Chen, K. Sarva, I. Siddiqui, R.K. Srivastava, Curcumin enhances the apoptosis-inducing potential of TRAIL in prostate cancer cells: molecular mechanisms of apoptosis, migration and angiogenesis, Journal of Molecular Signaling, 2 (2007) 10-10.

[4] A.L. Hilchie, S.J. Furlong, K. Sutton, A. Richardson, M.R. Robichaud, C.A. Giacomantonio, N.D. Ridgway, D.W. Hoskin, Curcumin-induced apoptosis in PC3 prostate carcinoma cells is caspase-independent and involves cellular ceramide accumulation and damage to mitochondria, Nutr Cancer, 62 (2010) 379-389.

[5] L. Camacho, O. Meca-Cortes, J.L. Abad, S. Garcia, N. Rubio, A. Diaz, T. Celia-Terrassa, F. Cingolani, R. Bermudo, P.L. Fernandez, J. Blanco, A. Delgado, J. Casas, G. Fabrias, T.M. Thomson, Acid ceramidase as a therapeutic target in metastatic prostate cancer, J Lipid Res, 54 (2013) 1207-1220.

[6] A.L. Cheng, C.H. Hsu, J.K. Lin, M.M. Hsu, Y.F. Ho, T.S. Shen, J.Y. Ko, J.T. Lin, B.R. Lin, W. Ming-Shiang, H.S. Yu, S.H. Jee, G.S. Chen, T.M. Chen, C.A. Chen, M.K. Lai, Y.S. Pu, M.H. Pan, Y.J. Wang, C.C. Tsai, C.Y. Hsieh, Phase I clinical trial of curcumin, a chemopreventive agent, in patients with high-risk or pre-malignant lesions, Anticancer Res, 21 (2001) 2895-2900.

[7] N. Dhillon, B.B. Aggarwal, R.A. Newman, R.A. Wolff, A.B. Kunnumakkara, J.L. Abbruzzese, C.S. Ng, V. Badmaev, R. Kurzrock, Phase II trial of curcumin in patients with advanced pancreatic cancer, Clin Cancer Res, 14 (2008) 4491-4499.

[8] A.C. Ketron, O.N. Gordon, C. Schneider, N. Osheroff, Oxidative metabolites of curcumin poison human type II topoisomerases, Biochemistry, 52 (2013) 221-227.

[9] M. Griesser, V. Pistis, T. Suzuki, N. Tejera, D.A. Pratt, C. Schneider, Autoxidative and cyclooxygenase-2 catalyzed transformation of the dietary chemopreventive agent curcumin, J Biol Chem, 286 (2011) 1114-1124.

[10] O.N. Gordon, C. Schneider, Vanillin and ferulic acid: not the major degradation products of curcumin, Trends Mol Med. 2012 Jul;18(7):361-3; author reply 363-4. doi: 10.1016/j.molmed.2012.04.011. Epub 2012 May 30.

[11] Y.J. Wang, M.H. Pan, A.L. Cheng, L.I. Lin, Y.S. Ho, C.Y. Hsieh, J.K. Lin, Stability of curcumin in buffer solutions and characterization of its degradation products, J Pharm Biomed Anal, 15 (1997) 1867-1876.

[12] E. Monti, R. Supino, M. Colleoni, B. Costa, R. Ravizza, M.B. Gariboldi, Nitroxide TEMPOL impairs mitochondrial function and induces apoptosis in HL60 cells, J Cell Biochem, 82 (2001) 271-276.

[13] J. Bouayed, T. Bohn, Exogenous antioxidants - Double-edged swords in cellular redox state: Health beneficial effects at physiologic doses versus deleterious effects at high doses, Oxid Med Cell Longev, 3 (2010) 228-237.

[14] K. Cho, X. Wang, S. Nie, Z.G. Chen, D.M. Shin, Therapeutic nanoparticles for drug delivery in cancer, Clin Cancer Res, 14 (2008) 1310-1316.

[15] P. Anand, H.B. Nair, B. Sung, A.B. Kunnumakkara, V.R. Yadav, R.R. Tekmal, B.B. Aggarwal, Design of curcumin-loaded PLGA nanoparticles formulation with enhanced cellular uptake, and increased bioactivity in vitro and superior bioavailability in vivo, Biochem Pharmacol, 79 (2010) 330-338.

[16] P. Verderio, P. Bonetti, M. Colombo, L. Pandolfi, D. Prosperi, Intracellular drug release from curcumin-loaded PLGA nanoparticles induces G2/M block in breast cancer cells, Biomacromolecules, 14 (2013) 672-682.

[17] B. Kumar, S. Koul, L. Khandrika, R.B. Meacham, H.K. Koul, Oxidative stress is inherent in prostate cancer cells and is required for aggressive phenotype, Cancer Res, 68 (2008) 1777-1785.

[18] Y. Matsumura, H. Maeda, A new concept for macromolecular therapeutics in cancer chemotherapy: mechanism of tumoritropic accumulation of proteins and the antitumor agent smancs, Cancer Res, 46 (1986) 6387-6392.

[19] T. Yoshitomi, Y. Ozaki, S. Thangavel, Y. Nagasaki, Redox nanoparticle therapeutics to cancer--increase in therapeutic effect of doxorubicin, suppressing its adverse effect, J Control Release, 172 (2013) 137-143.

[20] T. Yoshitomi, D. Miyamoto, Y. Nagasaki, Design of core--shell-type nanoparticles carrying stable radicals in the core, Biomacromolecules, 10 (2009) 596-601.

[21] S.Y. Kim, I.G. Shin, Y.M. Lee, C.S. Cho, Y.K. Sung, Methoxy poly(ethylene glycol) and epsilon-caprolactone amphiphilic block copolymeric micelle containing indomethacin. II. Micelle formation and drug release behaviours, J Control Release, 51 (1998) 13-22.

[22] T. Yoshitomi, R. Suzuki, T. Mamiya, H. Matsui, A. Hirayama, Y. Nagasaki, pH-sensitive radical-containing-nanoparticle (RNP) for the L-band-EPR imaging of low pH circumstances, Bioconjug Chem, 20 (2009) 1792-1798.

[23] M. Kamimura, T. Furukawa, S.-i. Akiyama, Y. Nagasaki, Enhanced intracellular drug delivery of pH-sensitive doxorubicin/poly(ethylene glycol)-block-poly(4-vinylbenzylphosphonate) nanoparticles in multi-drug resistant human epidermoid KB carcinoma cells, Biomaterials Science, 1 (2013) 361-367.

[24] P. Storz, Reactive oxygen species in tumor progression, Front Biosci, 10 (2005) 1881-1896.

[25] C.D. Chen, C.L. Sawyers, NF-kappa B activates prostate-specific antigen expression and is upregulated in androgen-independent prostate cancer, Mol Cell Biol, 22 (2002) 2862-2870.

[26] M. Uchiyama, T. Fischer, J. Mueller, M. Oguchi, N. Yamamura, H. Koda, H. Iwabuchi, T. Izumi, Identification of novel metabolic pathways of pioglitazone in hepatocytes: N-glucuronidation of thiazolidinedione ring and sequential ring-opening pathway, Drug Metab Dispos, 38 (2010) 946-956.